Self-organisation of zooplankton communities produces similar food chain lengths throughout the ocean

Jason Everett (jason.everett@uq.edu.au)
The University of Queensland https://orcid.org/0000-0002-6681-8054
Ryan Heneghan
Queensland University of Technology
Julia Blanchard
University of Tasmania https://orcid.org/0000-0003-0532-4824
Iain Suthers
University of New South Wales https://orcid.org/0000-0002-9340-7461
Evgeny Pakhomov
University of British Columbia
Patrick Sykes
University of Queensland https://orcid.org/0000-0002-8530-5932
David Schoeman
University of the Sunshine Coast https://orcid.org/0000-0003-1258-0885
Mark Baird
CSIRO https://orcid.org/0000-0003-4955-2298
Sünnje Linnéa Basedow
UiT The Arctic University of Norway https://orcid.org/0000-0001-6000-6090
Katarzyna Błachowiak-Samołyk
Polish Academy of Sciences
Michael Heath
University of Strathclyde
Russell Hopcroft
University of Alaska Fairbanks
Jenny Huggett
Fisheries and the Environment https://orcid.org/0000-0001-9315-8672
Martin Huret
IFREMER
David Kimmel
NOAA Fisheries, Alaska Fisheries Science Center https://orcid.org/0000-0001-7232-7801
Jean-Philippe Labat

Laboratoire d'Océanographie de Villefranche
Rubens Lopes
University of São Paulo
Catarina Marcolin
Federal University of Southern Bahia
Enrique Nogueira
Instituto Español de Oceanografía (IEO-CSIC) https://orcid.org/0000-0002-4222-928X
Margaux Noyon
Nelson Mandela University
Sabine Schultes
LMU Munich
Marc Sourisseau
IFREMER, French Institute for Sea Research
Kerrie Swadling
University of Tasmania
Emilia Trudnowska
Institute of Oceanology, Polish Academy of Sciences https://orcid.org/0000-0003-3471-6632
Anthony Richardson
The University of Queensland

Article

Keywords:

Posted Date: April 25th, 2022

DOI: https://doi.org/10.21203/rs.3.rs-1186379/v1

Self-organisation of zooplankton communities produces similar food chain lengths throughout the ocean

Jason D. Everett[1,2,3,*,#], Ryan F. Heneghan[4,#], Julia L. Blanchard[5], Iain M. Suthers[3,6], Evgeny A. Pakhomov[7,8,9], Patrick Sykes[1], David S. Schoeman[10,11], Mark E. Baird[12], Sünnje L. Basedow[13], Katarzyna Błachowiak-Samołyk[14], Michael R. Heath[15], Russell R. Hopcroft[16], Jenny A. Huggett[17,18], Martin Huret[19], David G. Kimmel[20], Jean-Philippe Labat[21], Rubens M. Lopes[22], Catarina R. Marcolin[23], Enrique Nogueira[24], Margaux Noyon[25], Sabine Schultes[26], Marc Sourisseau[27], Kerrie M. Swadling[5], Emilia Trudnowska[14], Anthony J. Richardson[1,2]

[1]School of Mathematics and Physics, University of Queensland, Brisbane, QLD, Australia

[2]CSIRO Oceans and Atmosphere, Queensland Biosciences Precinct, St Lucia, QLD, Australia

[3]Centre for Marine Science and Innovation, School of Biological, Earth and Environmental Sciences, University of New South Wales, Sydney, NSW, Australia

[4]School of Mathematical Sciences, Queensland University of Technology, Brisbane, QLD, Australia

[5]Institute of Marine and Antarctic Studies, University of Tasmania, Hobart, TAS, Australia

[6]Sydney Institute of Marine Science, Mosman, NSW, Australia

[7]Department of Earth, Ocean and Atmospheric Sciences, University of British Columbia, Vancouver, BC, Canada

[8]Institute for the Oceans and Fisheries, University of British Columbia, Vancouver, BC, Canada

[9]Hakai Institute, Heriot Bay, BC, Canada

[10]Global-Change Ecology Research Group, School of Science, Technology and Engineering, University of the Sunshine Coast, Maroochydore, QLD, Australia

[11]Centre for African Conservation Ecology, Department of Zoology, Nelson Mandela University, Port Elizabeth, South Africa

[12]CSIRO Oceans and Atmosphere, Castray Esplanade, Hobart, TAS, Australia

[13]Department of Arctic and Marine Biology, UiT The Arctic University of Norway, 9037 Tromsø, Norway

[14]Institute of Oceanology Polish Academy of Sciences, Sopot, Poland

[15]University of Strathclyde, Department of Mathematics and Statistics, 26 Richmond Street Glasgow G1 1XH, UK

[16]Institute of Marine Sciences, University of Alaska, Fairbanks, AK, USA

[17]Oceans and Coasts Research, Department of Forestry, Fisheries and the Environment, Private Bag X4390, Cape Town 8000, South Africa

[18]Department of Biological Sciences and Marine Research Institute, University of Cape Town, Private Bag X3, Rondebosch 7701, South Africa

[19]DECOD (Ecosystem Dynamics and Sustainability), IFREMER, INRAE, Institut Agro - Agrocampus Ouest, Brest, France

[20]Alaska Fisheries Science Center, National Marine Fisheries Service, NOAA, 7600 Sand Point Way NE, Seattle, WA 98115 USA

[21]Sorbonne Université, CNRS, Laboratoire d'Océanographie de Villefranche (UMR 7093), Villefranche-sur-mer, France

[22]Department of Biological Oceanography, Oceanographic Institute, University of São Paulo, São Paulo 05508-120, Brazil

[23]Environmental Sciences Training Center, Federal University of Southern Bahia (UFSB), Rodovia Porto Seguro - Eunápolis, BR-367, Km 10, Porto Seguro, Bahia, 45810-000, Brazil

[24]Instituto Español de Ocanografía (COV), Consejo Superior de Investigaciones Científicas (IEO-CSIC), Subida al Radio Faro 50, 36390-Vigo, Spain

[25]Department of Oceanography and Institute for Coastal and Marine Research, Nelson Mandela University, Gqeberha, 6001, South Africa

[26]Aquatic Ecology, Faculty of Biology, LMU Munich, Großhaderner Str. 2 82152 Planegg-Martinsried, Germany

[27]IFREMER, French Institute for Sea Research, DYNECO PELAGOS, 29280 Plouzané, France.

*Corresponding Author: Jason.Everett@uq.edu.au

[#]These authors contributed equally to this work

We dedicate this work to our colleague, collaborator and friend, Dr A. David McKinnon, who passed away before this work was finished

ABSTRACT

For over 50 years, the conceptualisation of low-nutrient oligotrophic systems having longer food chains and thus lower energy transfer to fish than their high-nutrient eutrophic counterparts[1] has achieved the status of an ecological paradigm. However, recent global assessments indicate global fish biomass could be much higher than previously thought[2–4], suggesting that our traditional understanding of food webs may need to be revisited. Here, we challenge the classical paradigm by exploring the role of zooplankton in food webs across the world's oceans. Using observed zooplankton size spectra, and output from a size-spectrum model that resolves nine zooplankton groups, we conclude that food chains in oligotrophic (low-nutrient) and eutrophic (high-nutrient) systems have similar lengths. We offer a compelling hypothesis to explain this emergent pattern: self-organisation of zooplankton groups across the global productivity gradient regulates food chain length. We find that in oligotrophic systems the increased carnivory and longer food chains are offset by relatively large gelatinous filter feeders eating the dominant small phytoplankton, resulting in shorter-than-expected food chains, but decreasing food quality for fish. Our findings highlight the pivotal role zooplankton play in regulating energy transfer. Better resolution of zooplankton groups, their feeding relationships and carbon content in models will increase our ability to estimate current global fish biomass [5], project future fish biomass under climate change[6–8], and provide more-robust forecasts of nutrient[9] and carbon cycling[10].

MAIN TEXT

Marine food webs support the harvest of 84-130 million tonnes of fish annually and feed billions of people[11]. Fish harvest is related to phytoplankton at the base of the food web[12], although weakly[8], strongly indicating that zooplankton – the key trophic link between phytoplankton and fish – might play a role [1].

The broadly-accepted paradigm in food-web ecology posits that energy transfer to fish is meagre in oligotrophic (low-nutrient) systems, with low phytoplankton biomass dominated by small phytoplankton, and a long food chain including flagellates, ciliates and carnivorous zooplankton, resulting in a greater number of trophic steps and a higher total metabolic energy loss[13–15] (Fig. 1a). By contrast, energy transfer is greater in eutrophic (high-nutrient) food webs, with high phytoplankton biomass and a short food chain with large herbivorous zooplankton as the sole intermediate step, resulting in lower energy loss[13] (Fig. 1a). This classical view[16] underpins conceptual theory and modelling [17,18], yet has not been tested globally.

Size-based theory provides a complementary perspective [5,15,19,20]. It postulates that energy transfer to fish is determined by trophic transfer efficiency and predator-prey mass ratios (PPMR) [15]. Although transfer efficiency is slightly higher in oligotrophic than eutrophic systems[7] its mean is ~10%[21,22], whereas PPMR, which determines the number of trophic steps and thus food chain length[19], can vary by orders of magnitude. For example, carnivorous zooplankton have low PPMRs (3-500)[5], resulting in the long food chains presumed in oligotrophic systems[15]. By contrast, herbivorous zooplankton have high PPMRs (13,000-16 million)[5], resulting in the short food chains assumed in eutrophic systems. This size-based perspective is represented by plotting biomass in equal logarithmic size intervals[19,23] (Fig. 1a). The y-intercept of the linear fit is higher in eutrophic systems because of greater phytoplankton biomass (Fig. 1a). Longer food chains in oligotrophic systems result in steeper slopes, reflecting the dominance of small phytoplankton, lower PPMRs and increased carnivory. By

contrast, flatter slopes in eutrophic systems reflect the greater dominance of larger phytoplankton, higher PPMRs, increased herbivory, and shorter food chains[24] (Fig. 1a). These contrasting slopes are well established for phytoplankton[14,25] and are hypothesised to continue through zooplankton to fish[19,23], although this remains unproven in the global ocean.

To test this hypothesis, we analysed zooplankton size measurements collected using optical plankton counters. We paired each observation with satellite-derived chlorophyll-*a*, a proxy for phytoplankton biomass, and analysed the size spectrum in oligotrophic (<0.1 $mg.m^{-3}$, n=10,764) and eutrophic (>1 $mg.m^{-3}$, n=9,555; Fig. S1) systems. As expected, there was a lower intercept (Fig. 1b) and thus lower mean (±SE) zooplankton biomass in oligotrophic (233±4 $mg.m^{-3}$) than eutrophic systems (1,606±90 $mg.m^{-3}$). However, contrary to expectations, the slope of the observed mean zooplankton size spectrum in each system (Fig. 1b) was close to the canonical -1 predicted by Sheldon et al.[23], with no significant difference in slopes between oligotrophic (-0.95) and eutrophic systems (-0.97, F=1.15, p=0.29, ANCOVA; Fig. 1b), implying comparable food-chain lengths and challenging the classical food-web view.

To investigate why zooplankton slopes might be similar in oligotrophic and eutrophic systems, we used the Zooplankton Model of Size Spectra (ZooMSS)[5]. ZooMSS is a global size-structured marine ecosystem model (1° resolution), representing phytoplankton to fish. It has three phytoplankton (pico-, nano- and micro-phytoplankton), nine zooplankton (flagellates, ciliates, omnivorous copepods, larvaceans, carnivorous copepods, chaetognaths, salps, euphausiids, jellyfish), and three fish groups (small, medium and large). Zooplankton and fish groups have three functional traits[19]: size, PPMR and carbon content (an index of food quality). Each cell was initialised with an identical zooplankton community. Zooplankton community composition emerges in each cell based on the relative competitiveness of each group to temperature and phytoplankton size structure[5](Fig. S2, S3).

Consistent with observations, we found size-spectrum slopes from ZooMSS were similar in oligotrophic (-0.93) and eutrophic systems (-0.96, F=0.88, p=0.35, ANCOVA; Fig. 1c), again implying similar food-chain lengths. Because ZooMSS captured similar patterns in size-spectrum slopes to observations (Fig. 1b,c) and reproduces global patterns in biomass, growth and distributions of zooplankton groups[5], we used it to explore potential explanations.

Major differences in the distribution of zooplankton groups emerged within ZooMSS across the global gradient of chlorophyll *a*, despite initialising each modelled spatial grid cell with an identical zooplankton community. Omnivores (euphausiids and omnivorous copepods) were more abundant in shelf, upwelling and polar regions (Fig. 2a, S4), consistent with observations[14,26,27]. By contrast, carnivores (carnivorous copepods, chaetognaths and jellyfish, Fig. 2b) and filter-feeders (larvaceans and salps; Fig. 2c) increased in importance in oligotrophic gyres, similar to observations[26,27]. These spatial shifts were a consequence of the relative fitness of each group in response to size-based feeding competition for the size-structured phytoplankton resource (Fig. S2). In eutrophic systems with large phytoplankton, omnivores dominate (Fig. 2e) because they feed efficiently on larger phytoplankton [28,29], outcompeting similar-sized filter-feeders (Fig. 2e) whose feeding structures become clogged when large cells are abundant[30–32]. Therefore, in eutrophic systems the primary pathway from phytoplankton to small fish is through omnivorous crustaceans, which consume 84% of the phytoplankton (Fig. 3b).

The pathway in oligotrophic systems is different (Fig. 2d). In these picophytoplankton-dominated systems, microzooplankton, carnivorous zooplankton and filter-feeders (Figs. 2e) become more important. Heterotrophic flagellates and ciliates[14,17], and the much-larger larvaceans and salps[30,32,33], feed on smaller phytoplankton unavailable to copepods and euphausiids[29](Fig. 2a,c). Consistent with conventional food-web theory, much of the production in oligotrophic systems passes through microzooplankton with low PPMR, before being consumed by omnivores. This additional trophic

step decreases the energy available to omnivores, forcing them to compete with carnivores for microzooplankton prey, causing omnivores to decline relative to filter-feeders and carnivores. The major link in these oligotrophic systems was therefore through filter-feeders, which consume 73% of the phytoplankton, while omnivores ingested only 23% (Fig. 3a, S5).

Despite contrasting trophic pathways in oligotrophic and eutrophic systems, ZooMSS surprisingly predicts that both systems have similar food-chain lengths (Fig. 3c). There is a mean of 2.4 trophic steps from phytoplankton to planktivorous fish in eutrophic systems and 2.6 steps in oligotrophic systems (Fig. 3c). When we remove filter feeders from the modelled food web, the mean trophic level in oligotrophic systems increases to 3.2 (Fig. 3c), and a more conventional food web emerges (Fig. S6). Since most traditional food-web models do not include filter feeders and rarely resolve zooplankton groups[34], these patterns would likely have remained hidden.

Our results challenge the classical paradigm that oligotrophic systems have substantially longer food chains than their eutrophic counterparts. ZooMSS suggests that similar food chain lengths are a consequence of shifts in community-wide PPMRs (Fig. 1a,b). Eutrophic systems had a mean PPMR of $10^{4.6}$, with peaks corresponding to carnivores, omnivorous copepods and euphausiids (Fig. 3f). Notably, oligotrophic systems had a similar mean PPMR of $10^{4.5}$, dominated by lower carnivore PPMRs, but largely offset by a broad peak of high PPMRs for filter-feeding larvaceans and salps (Fig. 3e). This implies a remarkable self-organisation of zooplankton feeding traits that gives rise to similar community-wide PPMRs, and thus similar mean size-spectrum slopes (Fig. 1) and food-chain lengths (Fig. 3c). This is contrary to classical food-web theory yet leads to the emergence of the "biomass equivalence rule" in the open ocean, based on an extension of size-spectrum theory[35].

Shorter-than-expected oligotrophic food chains could help explain how oceans might support higher fish biomass than previously thought (1.8–19.5 billion tonnes)[2–4]. Filter-feeders may play a role by

sustaining the vast mesopelagic fish biomass in tropical systems[36,37], which support valuable tuna fisheries. The ability of low-trophic position filter-feeders [17] to ingest picophytoplankton and bacteria could short-circuit the microbial loop, transferring carbon to larger sizes. However, traditional sampling techniques underestimate their role and almost no food-web models include filter-feeders[33,34,38]. Our findings highlight the unique, yet critical and overlooked role of filter-feeding zooplankton.

Although the different zooplankton groups occur throughout the ocean[26], our work suggests that there is a crustacean-gelatinous shift[39] across the chlorophyll-a gradient, which has fundamental implications for food webs. Zooplankton have three main body forms[40]: microzooplankton (flagellates and ciliates) are small and dense (high carbon content); crustaceans (copepods and euphausiids) are large and dense; and filter feeders (salps and larvaceans) are large and gelatinous (low carbon content). We show here that the relative success of these three discrete body forms changes in response to the chlorophyll *a* concentration and the phytoplankton size structure, and stabilises the food-chain length by diversifying the PPMR. However, this change also results in a reduced carbon content of zooplankton in oligotrophic waters, diminishing food quality for fish – zooplankton community-wide carbon content decreases from 12% in eutrophic waters to 6% in oligotrophic waters (Fig. 3d). The crustacean-gelatinous shift thus has important implications for the biomass of fish.

The crustacean-gelatinous shift also has implications for the food quality for fish and nutrient cycling[9,31,33]. Consistent with observations of active carbon flux[41], the greater importance of crustaceans in eutrophic regions (Fig. 2a,e) suggests carbon is rapidly shifted deeper through active transport by vertical migration[10]. The greater importance of filter-feeders in oligotrophic regions (Fig. 2c,e) suggests carbon is mainly shifted deeper passively, through sinking of mucous houses of larvaceans, which are shed up to 40 times per day per individual [31,33,42], and heavy faecal pellets of

salps[33,38], releasing bioavailable iron as they break down[9]. Zooplankton are gaining increasing recognition as important nutrient recyclers and our results elucidate how community self-organisation could regulate their role in the global carbon cycle. With the push to exploit mesopelagic fish, there is a need for improved understanding of the energy pathways through zooplankton – and an ability to model them[43].

Despite the importance of zooplankton groups, they are rarely included in biogeochemical, ecosystem, Earth-system or size-spectrum models[34]. To assess the impact on fish of better-representing zooplankton, we re-ran ZooMSS with a single generic zooplankton group (i.e. without differentiating their feeding traits and assuming a PPMR of 100; see Methods). Resolving zooplankton groups resulted in up to 272% more fish in some regions, with a mean of 79% more fish globally compared to estimates using a single zooplankton group (Fig. 4). Models not resolving zooplankton groups underestimate fish biomass[8] and the impact of climate change[24,44]. Ecosystem modelling has evolved to include more functional traits in phytoplankton[45] and fish[19], and a similar paradigm shift is needed for zooplankton.

By integrating the largest assembled dataset of zooplankton size spectra with our improved understanding of the role of different zooplankton groups in the transfer of energy to higher trophic levels[5,41,43], our findings challenge the current paradigm that oligotrophic systems have longer food chains. Our size-spectrum model offers a compelling hypothesis to explain this phenomenon: changes in zooplankton community composition stabilise food-chain length across the productivity gradient. An enhanced understanding of the ecosystem role of zooplankton, which constitute 40% of total marine biomass[20], should improve our ability to project future fish biomass under climate change[7,8] and deliver more-robust forecasts of nutrient cycling[9] and carbon sequestration[46].

Acknowledgements

This contribution was funded by Australian Research Council Discovery Projects DP150102656 and DP190102293. RFH was funded by an Australian Government Research Training Program Scholarship and the Spanish Ministry of Science, Innovation and Universities, through the Acciones de Programacion Conjunta Internacional (PCIN-2017-115). PS was supported by an Australian Government Research Training Program Scholarship. RRH datasets were funded through the Monterey Bay Aquarium Research Institute. DGK datasets were funded through grants from the US National Science Foundation and NOAA Coastal Ocean Program. SLB datasets were funded through grants from the Norwegian Research Council and the EU. MN and JAH thank Isabelle Ansorge, University of Cape Town, for the loan of the LOPC. LOPC datasets from Brazilian waters were made possible by grants from the National Council for Scientific and Technological Development (CNPq) to CRM (141409/2010-0, 141793/2012-0) and RML (420219/2005-6, 310642/2017-5). SS was supported by São Paulo Research Foundation (FAPESP), postdoctoral fellowship grant 06/06683-9. We acknowledge funding from the Research Computing Centre (RCC), University of Queensland. This research includes computations using the computational cluster Katana supported by Research Technology Services at UNSW Sydney. GlobColour data (http://globcolour.info) used in this study has been developed, validated, and distributed by ACRI-ST, France. The plankton silhouettes in Figure 1A are courtesy of the Integration and Application Network, University of Maryland Center for Environmental Science (ian.umces.edu/symbols/). We acknowledge the work of all the sea-going scientists and crew who made the collection of the zooplankton size data possible.

Author Contributions

JDE, RFH, AJR, EAP, JLB and IMS conceived the study; JDE and RFH ran the model simulations and conducted the analysis with help from AJR and PS. JDE, IMS, AJR, SS, RRH, EP, ET, DGK, MN, JAH, CRM, SLB, RML, KBS, MRH, MH, JPL, EN, MS, KMS and Dr A. David McKinnon contributed data to the database used in this analysis. JDE, RFH and AJR wrote the first version of the manuscript, and all authors contributed to the revisions.

Competing Interests

The authors declare no competing interests.

FIGURES

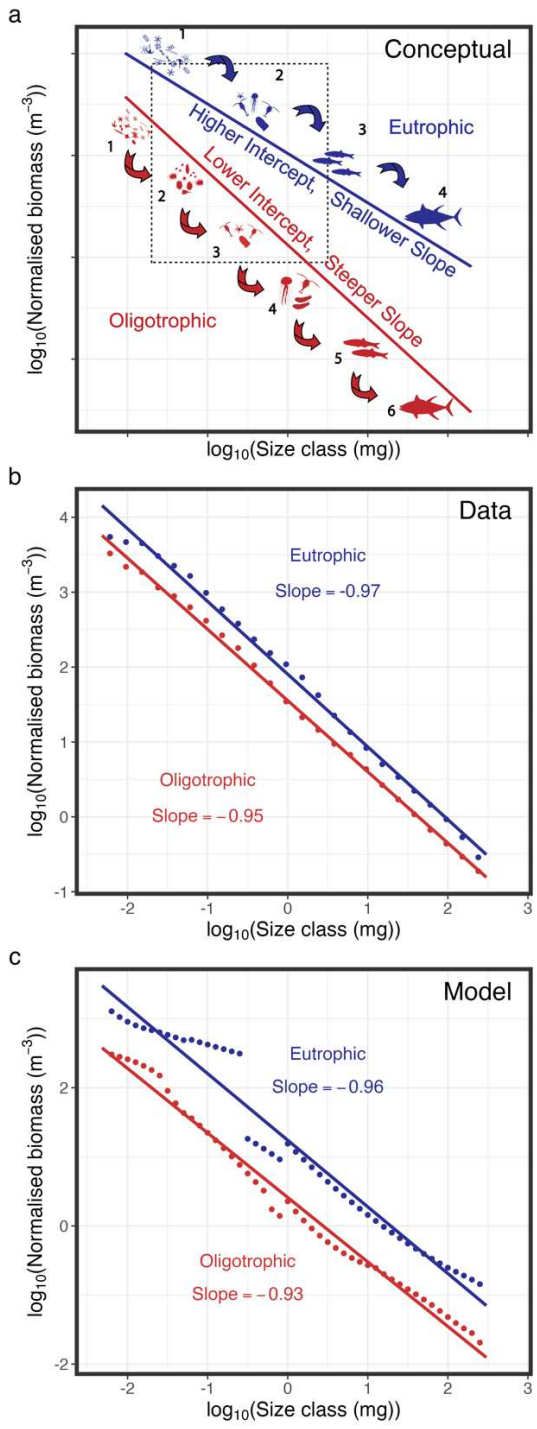

Figure 1: Size spectra of food webs.

a, Conceptual view integrating the size-based and classical views of food webs for eutrophic (top) and oligotrophic (bottom) systems (icons not drawn to scale). **b,** Observed normalised biomass size spectra of zooplankton from optical plankton data, showing similar slopes in eutrophic and oligotrophic systems. **c,** Modelled normalised biomass size spectra of zooplankton from ZooMSS, also showing similar slopes. The dashed box in **a** represents the approximate size-range of data in **b** and **c**.

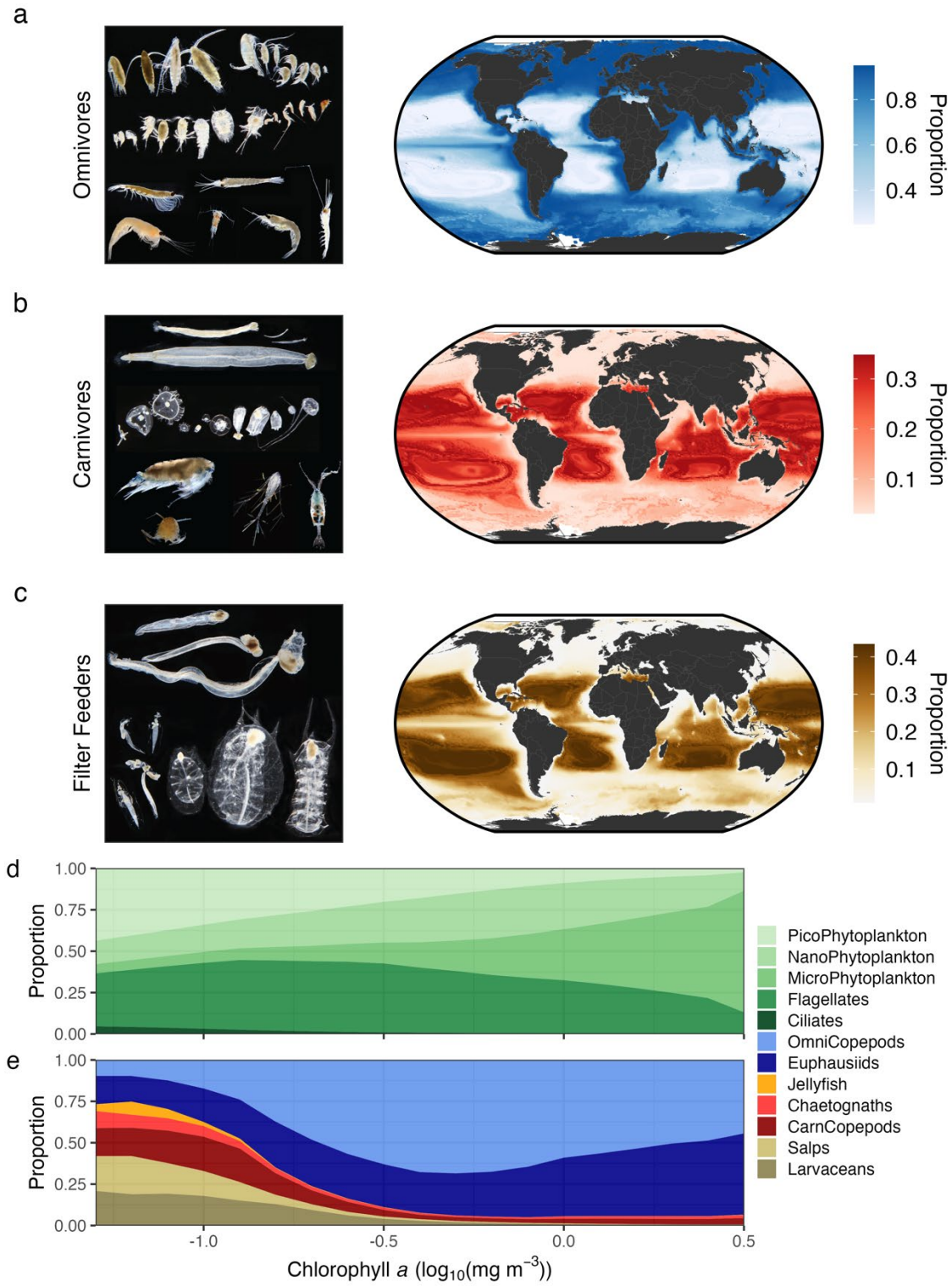

Figure 2: Composition of zooplankton groups in ZooMSS.

a-c, Spatial maps of the proportion of total zooplankton biomass for **(a)** Omnivores, **(b)** Carnivores, and **(c)** Filter feeders. See Figure S4 for maps of specific taxa. **d-e,** Proportion of biomass in **(d)** Phytoplankton and microzooplankton, and **(e)** Zooplankton across a chlorophyll *a* gradient. Photographs are for illustrative purposes only and are not to scale. Courtesy of Julian Uribe Palomino (CSIRO, Australia).

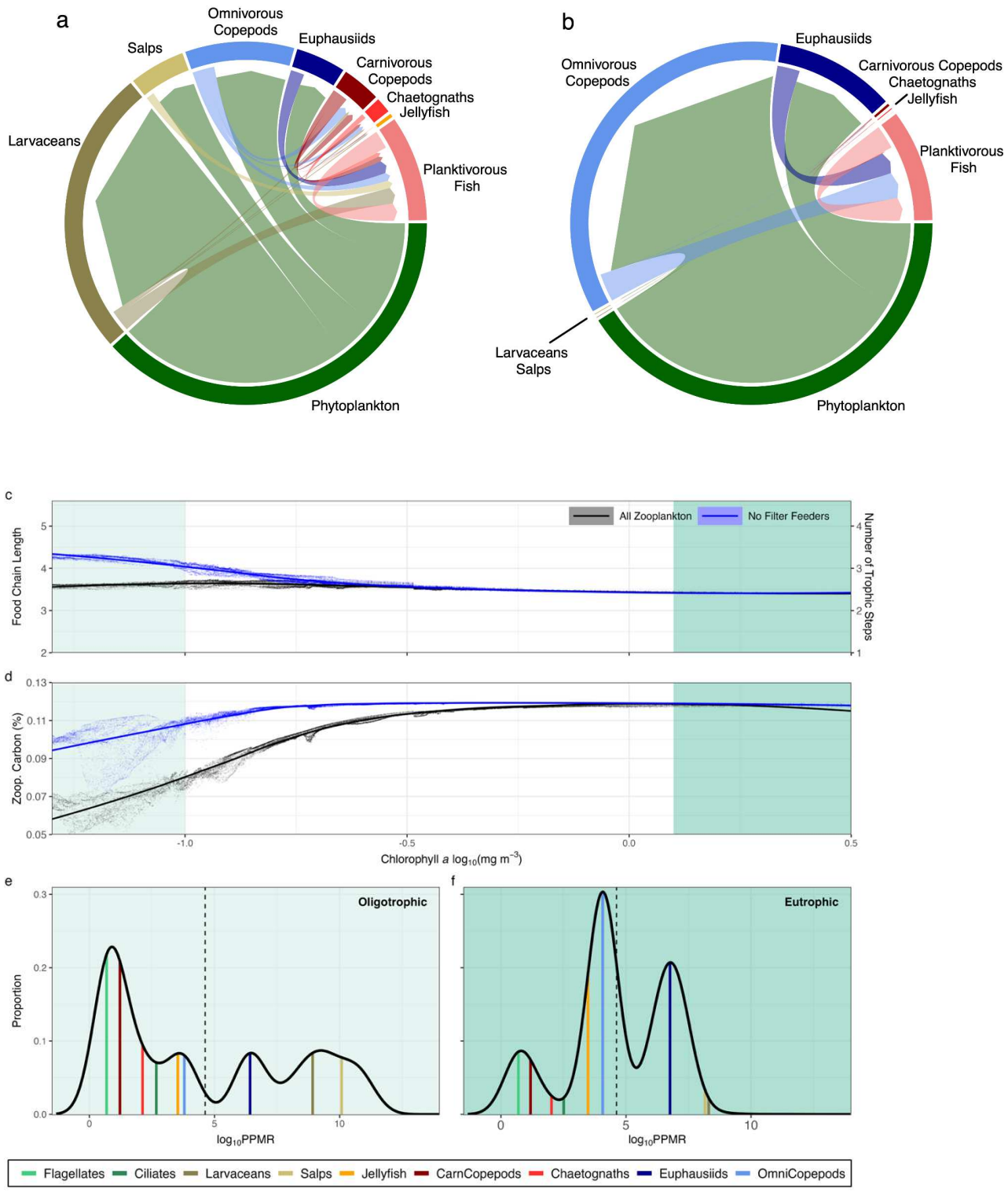

Figure 3: Output from ZooMSS showing changes in community composition and implications for food webs.

a, b, Circular food web diagrams showing biomass transfer in **(a)** Oligotrophic and **(b)** Eutrophic food webs, highlighting vastly different biomass pathways. Pathways through the food web can be discerned by following the coloured link from the prey (outer colour) to their predator. The width of the link corresponds to the proportion of biomass of prey consumed by its predator, and the width of

the outer band corresponds to the proportion of the model biomass. Food web structure including microzooplankton is shown in Fig. S5. **c,** Little change in food chain length (left) and average number of trophic steps (right) to planktivorous fish (1 = directly eating phytoplankton) across the chlorophyll *a* gradient (black) when compared to the change in trophic steps for a ZooMSS run with no filter feeders (blue). **d,** Lower carbon content of zooplankton in oligotrophic than eutrophic systems. **e**,**f,** Distributions of Predator-Prey Mass Ratios (PPMRs) in (e) Oligotrophic and (f) Eutrophic systems. Dashed line is the mean, which is similar in the two systems. Light and dark green shaded areas in **(c)-(f)** indicate limits of oligotrophic (0.1 mg m^{-3}) and eutrophic (1 mg m^{-3}) systems.

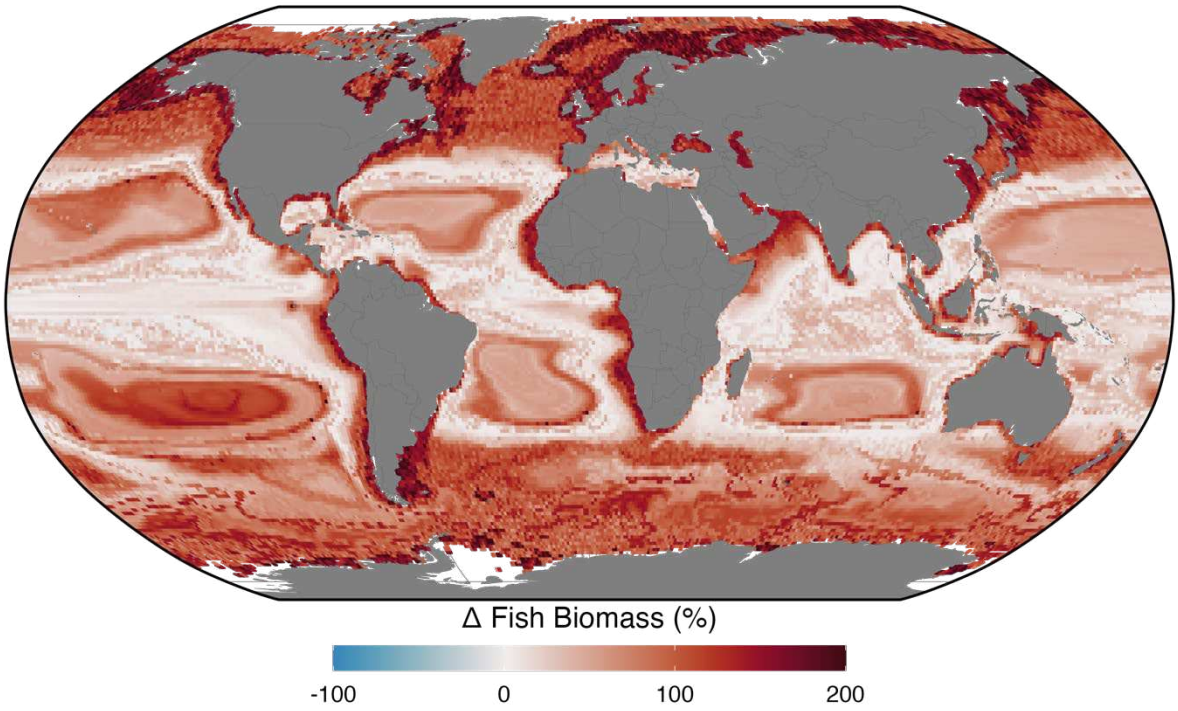

Figure 4: Change in total fish biomass when resolving zooplankton

Change in total fish biomass spatially when we include all 7 meso-zooplankton groups, compared to running ZooMSS with only a single generic zooplankton group.

References

1. Ryther, J. H. Photosynthesis and Fish Production in the Sea. *Science* **166**, 72–76 (1969).
2. Anderson, T. R. *et al.* Quantifying carbon fluxes from primary production to mesopelagic fish using a simple food web model. *ICES J. Mar. Sci.* **76**, 690–701 (2019).
3. Irigoien, X. *et al.* Large mesopelagic fishes biomass and trophic efficiency in the open ocean. *Nat. Commun.* **5**, 3271 (2014).
4. Proud, R., Handegard, N., Kloser, R., Cox, M. & Brierley, A. From siphonophores to deep scattering layers: uncertainty ranges for the estimation of global mesopelagic fish biomass. *ICES J. Mar. Sci.* **76**, 718–733 (2019).
5. Heneghan, R. F. *et al.* A functional size-spectrum model of the global marine ecosystem that resolves zooplankton composition. *Ecol. Model.* **435**, 109265 (2020).
6. Kwiatkowski, L., Aumont, O. & Bopp, L. Consistent trophic amplification of marine biomass declines under climate change. *Glob. Change Biol.* **25**, 218–229 (2019).
7. du Pontavice, H., Gascuel, D., Reygondeau, G., Maureaud, A. & Cheung, W. W. L. Climate change undermines the global functioning of marine food webs. *Glob. Change Biol.* **26**, 1306–1318 (2020).
8. Stock, C. A. *et al.* Reconciling fisheries catch and ocean productivity. *Proc. Natl. Acad. Sci.* **114**, E1441–E1449 (2017).
9. Böckmann, S. *et al.* Salp fecal pellets release more bioavailable iron to Southern Ocean phytoplankton than krill fecal pellets. *Curr. Biol.* **31**, 2737-2746.e3 (2021).
10. Hansen, A. N. & Visser, A. W. Carbon export by vertically migrating zooplankton: an optimal behavior model: Optimal vertical migration and carbon export. *Limnol. Oceanogr.* **61**, 701–710 (2016).
11. FAO. *The State of World Fisheries and Aquaculture 2020*. (FAO, 2020). doi:10.4060/ca9229en.

12. Chassot, E. *et al.* Global marine primary production constrains fisheries catches. *Ecol. Lett.* **13**, 495–505 (2010).
13. Armengol, L., Calbet, A., Franchy, G., Rodríguez-Santos, A. & Hernández-León, S. Planktonic food web structure and trophic transfer efficiency along a productivity gradient in the tropical and subtropical Atlantic Ocean. *Sci. Rep.* **9**, 2044 (2019).
14. Barton, A. D. *et al.* The biogeography of marine plankton traits. *Ecol. Lett.* **16**, 522–534 (2013).
15. Jennings, S. & Warr, K. J. Smaller predator-prey body size ratios in longer food chains. *Proc. R. Soc. Lond. B Biol. Sci.* **270**, 1413–1417 (2003).
16. Cushing, D. H. A difference in structure between ecosystems in strongly stratified waters and in those that are only weakly stratified. *J. Plankton Res.* **11**, 1–13 (1989).
17. Hunt, B. P. V. *et al.* Pelagic food web structure in high nutrient low chlorophyll (HNLC) and naturally iron fertilized waters in the Kerguelen Islands region, Southern Ocean. *J. Mar. Syst.* **224**, 103625 (2021).
18. Soviadan, Y. D. *et al.* Patterns of mesozooplankton community composition and vertical fluxes in the global ocean. *Prog. Oceanogr.* **200**, 102717 (2022).
19. Blanchard, J. L., Heneghan, R. F., Everett, J. D., Trebilco, R. & Richardson, A. J. From Bacteria to Whales: Using Functional Size Spectra to Model Marine Ecosystems. *Trends Ecol. Evol.* **32**, 174–186 (2017).
20. Hatton, I. A., Heneghan, R. F., Bar-On, Y. M. & Galbraith, E. D. The global ocean size-spectrum from bacteria to whales. *Sci. Adv.* **7**, eabh3732 (2021).
21. Barneche, D. R. *et al.* Warming impairs trophic transfer efficiency in a long-term field experiment. *Nature* **592**, 76–79 (2021).
22. Woodson, C. B., Schramski, J. R. & Joye, S. B. A unifying theory for top-heavy ecosystem structure in the ocean. *Nat. Commun.* **9**, 23 (2018).
23. Sheldon, R. W., Prakash, A. & Sutcliffe, W. H. The size distribution of particles in the ocean. *Limnol. Oceanogr.* **17**, 327–340 (1972).

24. Heneghan, R. F., Hatton, I. A. & Galbraith, E. D. Climate change impacts on marine ecosystems through the lens of the size spectrum. *Emerg. Top. Life Sci.* **3**, 233–243 (2019).
25. Barnes, C., Irigoien, X., De Oliveira, J. A. A., Maxwell, D. & Jennings, S. Predicting marine phytoplankton community size structure from empirical relationships with remotely sensed variables. *J. Plankton Res.* **33**, 13–24 (2011).
26. Brandão, M. *et al.* Macroscale patterns of oceanic zooplankton composition and size structure. *Sci. Rep.* **11**, 15714 (2021).
27. McGinty, N., Barton, A., Record, N., Finkel, Z. & Irwin, A. Traits structure copepod niches in the North Atlantic and Southern Ocean. *Mar. Ecol. Prog. Ser.* **601**, 109–126 (2018).
28. Berggreen, U., Hansen, B. & Kiørboe, T. Food size spectra, ingestion and growth of the copepod *Acartia tonsa* during development: Implications for determination of copepod production. *Mar. Biol.* **99**, 341–352 (1988).
29. Fuchs, H. & Franks, P. Plankton community properties determined by nutrients and size-selective feeding. *Mar. Ecol. Prog. Ser.* **413**, 1–15 (2010).
30. Alldredge, A. L. Abandoned Larvacean Houses: A Unique Food Source in the Pelagic Environment. *Science* **177**, 885–887 (1972).
31. Katija, K., Sherlock, R. E., Sherman, A. D. & Robison, B. H. New technology reveals the role of giant larvaceans in oceanic carbon cycling. *Sci. Adv.* **3**, e1602374 (2017).
32. Sutherland, K. R. & Madin, L. P. A comparison of filtration rates among pelagic tunicates using kinematic measurements. *Mar. Biol.* **157**, 755–764 (2010).
33. Sutherland, K. R. & Thompson, A. W. Pelagic tunicate grazing on marine microbes revealed by integrative approaches. *Limnol. Oceanogr.* **67**, 102–121 (2022).
34. Everett, J. D. *et al.* Modeling What We Sample and Sampling What We Model: Challenges for Zooplankton Model Assessment. *Front. Mar. Sci.* **4**, (2017).
35. Polishchuk, L. V. & Blanchard, J. L. Uniting Discoveries of Abundance-Size Distributions from Soils and Seas. *Trends Ecol. Evol.* **34**, 2–5 (2019).

36. Choy, C. A., Popp, B., Hannides, C. & Drazen, J. Trophic structure and food resources of epipelagic and mesopelagic fishes in the North Pacific Subtropical Gyre ecosystem inferred from nitrogen isotopic compositions: Trophic structure of pelagic fishes. *Limnol. Oceanogr.* **60**, 1156–1171 (2015).

37. Olivar, M. P. *et al.* Mesopelagic fishes across the tropical and equatorial Atlantic: Biogeographical and vertical patterns. *Prog. Oceanogr.* **151**, 116–137 (2017).

38. Henschke, N., Everett, J. D., Richardson, A. J. & Suthers, I. M. Rethinking the Role of Salps in the Ocean. *Trends Ecol. Evol.* **31**, 720–733 (2016).

39. Bode, A., Álvarez-Ossorio, M. T., Miranda, A. & Ruiz-Villarreal, M. Shifts between gelatinous and crustacean plankton in a coastal upwelling region. *ICES J. Mar. Sci.* **70**, 934–942 (2013).

40. Dölger, J., Kiørboe, T. & Andersen, A. Dense Dwarfs versus Gelatinous Giants: The Trade-Offs and Physiological Limits Determining the Body Plan of Planktonic Filter Feeders. *Am. Nat.* **194**, E30–E40 (2019).

41. Hernández-León, S. *et al.* Large deep-sea zooplankton biomass mirrors primary production in the global ocean. *Nat. Commun.* **11**, 6048 (2020).

42. Sato, R., Tanaka, Y. & Ishimaru, T. Species-specific house productivity of appendicularians. *Mar. Ecol. Prog. Ser.* **259**, 163–172 (2003).

43. Clerc, C., Aumont, O. & Bopp, L. Should we account for mesozooplankton reproduction and ontogenetic growth in biogeochemical modeling? *Theor. Ecol.* (2021) doi:10.1007/s12080-021-00519-5.

44. Woodworth-Jefcoats, P. A., Polovina, J. J. & Drazen, J. C. Climate change is projected to reduce carrying capacity and redistribute species richness in North Pacific pelagic marine ecosystems. *Glob. Change Biol.* **23**, 1000–1008 (2017).

45. Ward, B. A., Dutkiewicz, S., Jahn, O. & Follows, M. J. A size-structured food-web model for the global ocean. *Limnol. Oceanogr.* **57**, 1877–1891 (2012).

46. Pauli, N. *et al.* Krill and salp faecal pellets contribute equally to the carbon flux at the Antarctic Peninsula. *Nat. Commun.* **12**, 7168 (2021).

METHODS SUMMARY

Zooplankton Size Data

Zooplankton size data were extracted from a database of 123,407 size-spectra observations measured from 586 million individual zooplankton (see Data Availability below). The zooplankton sizes were measured using optical plankton counters – both LED Optical Plankton Counters (OPC)[47] and the Laser Optical Plankton Counter (LOPC)[48] – which were deployed in all ocean basins and across all seasons. The particles counted by the OPC/LOPC include not just live zooplankton, but also detritus and marine snow (aggregates)[47–50], which can at times be more abundant than zooplankton[51]. Methods have been developed in an attempt to distinguish between zooplankton and aggregates for the LOPC[49,52–54], however these methods cannot be applied to OPC measurements and therefore to be consistent we do not apply them here. Despite this, optical plankton counters compare reasonably well with data sets acquired with other sampling strategies, such as acoustics[55], plankton imaging instruments[56], and plankton nets[57,58] notwithstanding intrinsic limitations of each method[59].

Using code developed in this project (see Code Availability below), the raw outputs from each tow were processed in MATLAB R2021a (Mathworks Inc.). The size range of particles analysed were restricted to between 0.25 and 12 mm Equivalent Spherical Diameter (ESD) to ensure total overlap of sizes between the two instruments. The ESD was converted to biomass (expressed as wet-weight) by calculating the ellipsoid body volume (3:1 ratio of major:minor axis) and assuming individual particles have a near-neutral density of 1000 kg m^{-3} [60,61]. The biomass of each tow was standardised by the volume of the tow. To estimate nutrient status, each observation was paired with monthly satellite-derived chlorophyll *a* (GlobColour[62]), as a proxy for phytoplankton biomass[63], which was used to separate the data into oligotrophic (<0.1 mg chlorophyll *a* m^{-3}, n=10,764) and eutrophic categories (>1 mg chlorophyll *a* m^{-3}, n=9,555). Here we only analyse epipelagic (<200 m) data (Fig. S1).

Zooplankton Model of Size Spectrum (ZooMSS)

To investigate how different zooplankton groups might regulate energy transfer efficiency, we used the Zooplankton Model of Size Spectra (ZooMSS)[5]. ZooMSS is a functional size spectrum model[19] that represents the global marine ecosystem from phytoplankton through zooplankton to fish. ZooMSS has nine dynamic zooplankton and three fish groups (small, medium and large), and a single static phytoplankton community. The nine zooplankton groups are: heterotrophic flagellates and heterotrophic ciliates (microzooplankton); omnivorous copepods and euphausiids (omnivores); carnivorous copepods, chaetognaths and jellyfish (carnivores); and larvaceans and salps (filter feeders). These groups are the most abundant zooplankton in the ocean. Zooplankton and fish groups are represented in the model by their body-size ranges, size-based feeding characteristics, and carbon content (% of wet weight biomass). Abundances of the zooplankton and fish communities are driven by size-dependent processes of growth and mortality, with the temporal dynamics of each functional group governed by separate second- order McKendrick-von Foerster equations. A full overview of ZooMSS can be found in Heneghan et al.[5].

Across the global ocean, ZooMSS is initialised with an identical zooplankton community in 1° grid cells. The model is then run to equilibrium with a 500-year burn-in period and a weekly time-step, using mean annual sea surface temperature and chlorophyll *a* concentration estimated from satellite (2003-2018) as environmental drivers (Fig. S2). For each 1° grid cell, temperature affects rates of feeding and mortality in the zooplankton and fish communities, while chlorophyll *a* is used to calculate total phytoplankton biomass and the relative proportion of pico-, nano- and micro-phytoplankton (Fig. S3), using existing empirical relationships. Phytoplankton biomass is calculated from chlorophyll *a* using Marañón et al. [64] and the relative proportions of pico-, nano- and micro-phytoplankton are calculated from chlorophyll *a* using Brewin et al.[65]. These relative proportions are then used to calculate the slope, intercept and maximum size of the static phytoplankton community,

which serves as food for the zooplankton. Zooplankton community composition emerges in each grid cell depending on the relative fitness of the nine groups, arising from differences in their functional traits and environmental conditions (sea-surface temperature and phytoplankton community characteristics, from chlorophyll *a* concentration). With this simple implementation, ZooMSS can reproduce the major global patterns in zooplankton biomass and abundance of different groups, and produces sensible growth rate estimates for different groups[5].

To assess the importance of filter feeders in the marine food web, we removed salps and larvaceans from ZooMSS, keeping all other groups consistent (Fig. 3c,d, Fig. S6). Additionally, to examine the impact of better representing zooplankton groups on estimates of fish biomass (Fig. 4), we also ran ZooMSS with a single generic zooplankton group (i.e. without differentiating their feeding traits and assuming a PPMR of 100 and Carbon-Wet Weight Ratio of 0.1)[66,67]. All other model parameters remained the same.

Caveats of ZooMSS

Caveats associated with ZooMSS are described in detail in Heneghan et al.[5], and briefly summarised here. First, as ZooMSS is designed to explore steady-state conditions of marine ecosystems across environmental gradients, we have made simplifying assumptions about dynamic processes such as reproduction and seasonality. Zooplankton reproductive strategies are extremely complex and are typically ignored in models[66]. Fish-focused global models resolve reproduction explicitly in fish (but not in zooplankton)[68–70], whereas ZooMSS assumes constant recruitment. However, since many zooplankton groups time their reproduction to coincide with phytoplankton blooms [71,72] seasonal cycles of boom and bust in the phytoplankton is a major driver of variation of zooplankton productivity, particularly in polar and temperate areas. However, we smooth over these processes by using a yearly temporal resolution and assessing the long-term steady state zooplankton community. Second, ZooMSS assumes no movement of fish or plankton. Although most global fish-focused

models similarly assume no movement[68–70], others do[73,74]. Thus, each 1° grid cell in ZooMSS is run independently, which could bias abundances in certain regions due to movement of plankton by currents or apex predators by swimming. However, since most zooplankton and small fish are unlikely to travel the tens of kilometres required to move between 1° cells within their lifespans, we expect this to have a minor impact on our results. Third, ZooMSS does not incorporate phytoplankton dynamics, similar to many existing global marine ecosystem models[69,70,74–77], instead representing primary producers as a static abundance spectrum with slope, intercept and maximum size determined by annual mean chlorophyll *a*. This means that nutrient cycling and the impact of grazing on phytoplankton are not included. However, satellite chlorophyll *a* represents the net amount of phytoplankton present in response to processes such as nutrient cycling and grazing. Since ZooMSS was able to reproduce global zooplankton biomass and growth rates in the range of empirical estimates[5], we believe a static phytoplankton resource spectrum for zooplankton in each grid cell is a reasonable compromise between realism and model complexity. Fourth, effects of sea surface temperature were incorporated in the model as a multiplier on growth and mortality, with the same temperature scaling (here Q_{10}=2) used for all functional groups, which is a common assumption in models[78]. Although there is empirical evidence that different zooplankton species have different temperature scaling[79,80], we are unaware of a meta-analysis for temperature dependence of different processes for the broad taxonomic groups we use here. Fifth, we use chlorophyll *a* rather than primary production to drive ZooMSS. We do this because the functional groups in ZooMSS are all based on biomass, and chlorophyll *a* is a reasonable proxy for phytoplankton biomass[81]. Because small cells dominate in oligotrophic water[14], and growth is faster in warmer than colder waters[82], using chlorophyll *a* rather than net primary production likely underestimates the importance of picophytoplankton in the warm oligotrophic regions of the ocean, and thus the role of filter-feeders that can access them. Last, ZooMSS has been developed as an epipelagic model by including phytoplankton and zooplankton groups in the top 200 m, but it in a sense provides estimates of total zooplankton and fish biomass in the ocean. This is because ZooMSS is driven by chlorophyll *a* from

satellite, and phytoplankton are the dominant primary producers in the ocean. And because ZooMSS is not depth-resolved, there is no passive transport of carbon through sinking or active transport through diel vertical migration to deeper layers, so carbon is only lost from by metabolism[5].

Normalised Biomass Size Spectra

The Normalised Biomass Size Spectra (NBSS) for the observational and modelled data were calculated by binning the data into a series of logarithmically equal size intervals[83,84]. The binned data for each sample (observations) and grid-cell (ZooMSS), for each of the eutrophic and oligotrophic systems, were averaged to create a biomass size spectrum for each system and data source. This biomass size spectrum was then normalised by dividing the biomass of each bin by the width of the bin (mg m^{-3}/ mg). The NBSS is thus independent of any specified body-size interval, facilitating comparison across different studies and systems[85]. The slope of the NBSS was derived by fitting a least-squares linear regression to the normalised biomass size spectrum[83]. To test the differences in size spectrum slopes between oligotrophic and eutrophic systems, we used ANCOVA, with the Normalised log_{10}-transformed Biomass Size Spectrum (NBSS) as the response and a factor for System (Eutrophic and Oligotrophic as levels) and log_{10}-transformed mass bins as a continuous predictor.

Biomass Proportion Analysis

The proportion of phytoplankton (Fig 2d, S3a-c), microzooplankton (Fig. S3d,e) and mesozooplankton (Fig. 2a-c,e; Fig. S4) biomass were computed by calculating the proportion of biomass in each group (e.g. chaetognaths) from the summed total biomass of each category (e.g. mesozooplankton). For mapping, this was calculated on each grid-cell individually. For the chlorophyll *a* gradient, a distribution of log_{10}Chlorophyll *a* values were computed at 0.1 intervals between -1.7 and 0.5 log_{10}Chlorophyll *a* (n = 23) and the mean proportion calculated for each of the bins.

Food Web Analysis

Trophic levels and food chain length

The average trophic level of functional group i (TL_i) in each 1° grid cell was calculated by solving:

$$TL_i = 1 + \sum_j TL_j PD_{ij},$$

where TL_j is the trophic level of group j, and PD_{ij} is the proportion of the diet of group i, that comes from group j:

$$PD_{ij} = \frac{F_{ij}}{\sum_j F_{ij}},$$

and F_{ij} is the total biomass from group j consumed by group i (g yr^{-1}). Except for phytoplankton, which at the base of the food chain and has a fixed trophic level of 1, the trophic level of the different groups changes with diet, so for each simulation we used the Gauss-Jacobi iteration method to solve TL_i for each zooplankton and fish group[86]. The number of trophic steps in the food chain from phytoplankton to group i is thus $TL_i - 1$.

Zooplankton community carbon content

For each 1° grid cell, the carbon content of the zooplankton community, CC_Z, was:

$$CC_Z = \frac{C_j B_j}{\sum_j C_j B_j},$$

where B_j is the wet weight biomass of group j (g m^{-3}) and C_j is the carbon content of group j, as a proportion of wet biomass.

Predator-prey mass ratio distributions

The distributions of zooplankton predator-prey mass ratios (PPMRs) in oligotrophic (<0.1 mg m^{-3} chlorophyll *a*) and eutrophic regions (>1 mg m^{-3} chlorophyll *a*) were calculated by deriving the probability density function of zooplankton PPMRs, $P(z)$:

$$P(z) = \frac{zB_z}{B_{tot}},$$

where z is a PPMR from the range of zooplankton PPMRs, $P(z)$ is the probability of PPMR z, B_z is the total biomass of all zooplankton with a PPMR of z, and B_{tot} is the total biomass of all zooplankton.

Planktonic food-webs

The circular food web diagrams showing biomass transfer were calculated using the package circlize[87] in R and derived from the biomass and diets of the phytoplankton, zooplankton and planktivorous (small) fish in ZooMSS. Pathways through the food web can be discerned by following the coloured link from the prey to their predator. The width of the link corresponds to the proportion of biomass of prey consumed by its predator, and the width of the outer band for each group corresponds to its proportion of total biomass.

Coding environment

All analysis for this manuscript was completed using R 4.1.0 [88].

Data availability

Size Spectra Data: Everett et al. (in prep; *Scientific Data*); currently available from the corresponding author on request.

Model Output: The ZooMSS output generated during the current study are available from the corresponding author on request.

Code availability

ZooMSS Code: https://github.com/MathMarEcol/ZoopModelSizeSpectra

Analysis Code: https://github.com/MathMarEcol/FoodWebEfficiency

References (Methods)

47. Herman, A. W. Design and calibration of a new optical plankton counter capable of sizing small zooplankton. *Deep Sea Res. Part Oceanogr. Res. Pap.* **39**, 395–415 (1992).
48. Herman, A. W. The next generation of Optical Plankton Counter: the Laser-OPC. *J. Plankton Res.* **26**, 1135–1145 (2004).
49. Espinasse, B. *et al.* Conditions for assessing zooplankton abundance with LOPC in coastal waters. *Prog. Oceanogr.* **163**, 260–270 (2018).
50. Trudnowska, E., Sagan, S. & Błachowiak-Samołyk, K. Spatial variability and size structure of particles and plankton in the Fram Strait. *Prog. Oceanogr.* **168**, 1–12 (2018).
51. Trudnowska, E. *et al.* Marine snow morphology illuminates the evolution of phytoplankton blooms and determines their subsequent vertical export. *Nat. Commun.* **12**, 2816 (2021).
52. Checkley, D. M. *et al.* Assessing plankton and other particles in situ with the SOLOPC. *Limnol. Oceanogr.* **53**, 2123–2136 (2008).
53. Jackson, G. A. & Checkley, D. M. Particle size distributions in the upper 100m water column and their implications for animal feeding in the plankton. *Deep Sea Res. Part Oceanogr. Res. Pap.* **58**, 283–297 (2011).
54. Petrik, C. M., Jackson, G. A. & Checkley, D. M. Aggregates and their distributions determined from LOPC observations made using an autonomous profiling float. *Deep Sea Res. Part Oceanogr. Res. Pap.* **74**, 64–81 (2013).
55. Trudnowska, E. *et al.* Multidimensional zooplankton observations on the northern West Spitsbergen Shelf. *J. Mar. Syst.* **98–99**, 18–25 (2012).

56. Basedow, S. L., Tande, K. S., Norrbin, M. F. & Kristiansen, S. A. Capturing quantitative zooplankton information in the sea: Performance test of laser optical plankton counter and video plankton recorder in a Calanus finmarchicus dominated summer situation. *Prog. Oceanogr.* **108**, 72–80 (2013).

57. Everett, J. D., Baird, M. E. & Suthers, I. M. Three-dimensional structure of a swarm of the salp *Thalia democratica* within a cold-core eddy off southeast Australia. *J. Geophys. Res.* **116**, C12046 (2011).

58. Schultes, S. & Lopes, R. M. Laser Optical Plankton Counter and Zooscan intercomparison in tropical and subtropical marine ecosystems: LOPC and Zooscan intercomparison. *Limnol. Oceanogr. Methods* **7**, 771–784 (2009).

59. Marcolin, C. R., Lopes, R. M. & Jackson, G. A. Estimating zooplankton vertical distribution from combined LOPC and ZooScan observations on the Brazilian Coast. *Mar. Biol.* **162**, 2171–2186 (2015).

60. Finlay, K., Beisner, B. E. & Barnett, A. J. D. The use of the Laser Optical Plankton Counter to measure zooplankton size, abundance, and biomass in small freshwater lakes: LOPC in freshwater lakes. *Limnol. Oceanogr. Methods* **5**, 41–49 (2007).

61. Suthers, I. M., Taggart, C. T., Kelley, D., Rissik, D. & Middleton, J. H. Entrainment and advection in an island's tidal wake, as revealed by light attenuance, zooplankton, and ichthyoplankton. *Limnol. Oceanogr.* **49**, 283–296 (2004).

62. Garnesson, P., Mangin, A., Fanton d'Andon, O., Demaria, J. & Bretagnon, M. The CMEMS GlobColour chlorophyll *a* product based on satellite observation: multi-sensor merging and flagging strategies. *Ocean Sci.* **15**, 819–830 (2019).

63. Morel, A. & Maritorena, S. Bio-optical properties of oceanic waters: A reappraisal. *J. Geophys. Res. Oceans* **106**, 7163–7180 (2001).

64. Marañón, E. *et al.* Resource Supply Overrides Temperature as a Controlling Factor of Marine Phytoplankton Growth. *PLoS ONE* **9**, e99312 (2014).

65. Brewin, R. J. W. *et al.* Influence of light in the mixed-layer on the parameters of a three-component model of phytoplankton size class. *Remote Sens. Environ.* **168**, 437–450 (2015).

66. Andersen, K. H., Jacobsen, N. S. & Farnsworth, K. D. The theoretical foundations for size spectrum models of fish communities. *Can. J. Fish. Aquat. Sci.* **73**, 575–588 (2016).

67. Heneghan, R. F., Everett, J. D., Blanchard, J. L. & Richardson, A. J. Zooplankton Are Not Fish: Improving Zooplankton Realism in Size-Spectrum Models Mediates Energy Transfer in Food Webs. *Front. Mar. Sci.* **3**, (2016).

68. Blanchard, J. L., Law, R., Castle, M. D. & Jennings, S. Coupled energy pathways and the resilience of size-structured food webs. *Theor. Ecol.* **4**, 289–300 (2011).

69. Carozza, D. A., Bianchi, D. & Galbraith, E. D. The ecological module of BOATS-1.0: a bioenergetically-constrained model of marine upper trophic levels suitable for studies of fisheries and ocean biogeochemistry. *Geosci Model Dev* **9**, 1545–1565 (2016).

70. Petrik, C. M., Stock, C. A., Andersen, K. H., van Denderen, P. D. & Watson, J. R. Bottom-up drivers of global patterns of demersal, forage, and pelagic fishes. *Prog. Oceanogr.* **176**, 102124 (2019).

71. Atkinson, A. *et al.* Zooplankton response to a phytoplankton bloom near South Georgia, Antarctica. *Mar. Ecol. Prog. Ser.* **144**, 195–210 (1996).

72. Falkowski, P. G., Barber, R. T. & Smetacek, V. Biogeochemical Controls and Feedbacks on Ocean Primary Production. *Science* **281**, 200–206 (1998).

73. Cheung, W. W. L., Dunne, J., Sarmiento, J. L. & Pauly, D. Integrating ecophysiology and plankton dynamics into projected maximum fisheries catch potential under climate change in the Northeast Atlantic. *ICES J. Mar. Sci.* **68**, 1008–1018 (2011).

74. Maury, O. An overview of APECOSM, a spatialized mass balanced “Apex Predators ECOSystem Model” to study physiologically structured tuna population dynamics in their ecosystem. *Prog. Oceanogr.* **84**, 113–117 (2010).

75. Blanchard, J. L. *et al.* How does abundance scale with body size in coupled size-structured food webs? *J. Anim. Ecol.* **78**, 270–280 (2009).

76. Christensen, V. *et al.* The global ocean is an ecosystem: simulating marine life and fisheries: Modelling life and fisheries in the global ocean. *Glob. Ecol. Biogeogr.* **24**, 507–517 (2015).

77. Jennings, S. & Collingridge, K. Predicting Consumer Biomass, Size-Structure, Production, Catch Potential, Responses to Fishing and Associated Uncertainties in the World's Marine Ecosystems. *PLOS ONE* **10**, e0133794 (2015).

78. Kearney, K. A. *et al.* Using Global-Scale Earth System Models for Regional Fisheries Applications. *Front. Mar. Sci.* **8**, 622206 (2021).

79. Hansen, P. J., Bjørnsen, P. K. & Hansen, B. W. Zooplankton grazing and growth: Scaling within the 2-2,000-µm body size range. *Limnol Ocean.* **42**, 687–704 (1997).

80. Kiørboe, T. & Hirst, A. G. Shifts in Mass Scaling of Respiration, Feeding, and Growth Rates across Life-Form Transitions in Marine Pelagic Organisms. *Am. Nat.* **183**, E118–E130 (2014).

81. Cullen, J. J. The Deep Chlorophyll Maximum: Comparing Vertical Profiles of Chlorophyll *a*. *Can. J. Fish. Aquat. Sci.* **39**, 791–803 (1982).

82. Brown, J. H., Gillooly, J. F., Allen, A. P., Savage, V. M. & West, G. B. Toward a metabolic theory of ecology. *Ecology* **85**, 1771–1789 (2004).

83. Edwards, A. M., Robinson, J. P. W., Plank, M. J., Baum, J. K. & Blanchard, J. L. Testing and recommending methods for fitting size spectra to data. *Methods Ecol. Evol.* **8**, 57–67 (2017).

84. Sprules, W. G. & Barth, L. E. Surfing the biomass size spectrum: some remarks on history, theory, and application. *Can. J. Fish. Aquat. Sci.* **73**, 477–495 (2016).

85. Sprules, W. G. & Munawar, M. Plankton Size Spectra in Relation to Ecosystem Productivity, Size, and Perturbation. *Can. J. Fish. Aquat. Sci.* **43**, 1789–1794 (1986).

86. Sauer, M. J., Roesler, C. S., Werdell, P. J. & Barnard, A. Under the hood of satellite empirical chlorophyll a algorithms: revealing the dependencies of maximum band ratio algorithms on inherent optical properties. *Opt. Express* **20**, 20920 (2012).

87. Gu, Z., Gu, L., Eils, R., Schlesner, M. & Brors, B. circlize implements and enhances circular visualization in R. *Bioinformatics* **30**, 2811–2812 (2014).

88. R Core Team. *R: A Language and Environment for Statistical Computing*. (R Foundation for Statistical Computing, 2021).

89. Wirtz, K. Who is eating whom? Morphology and feeding type determine the size relation between planktonic predators and their ideal prey. *Mar. Ecol. Prog. Ser.* **445**, 1–12 (2012).

90. Menden-Deuer, S. & Lessard, E. J. Carbon to volume relationships for dinoflagellates, diatoms, and other protist plankton. *Limnol. Oceanogr.* **45**, 569–579 (2000).

91. Deibel, D. Feeding and metabolism of Appendicularia. in *The biology of pelagic tunicates* 139–149 (Oxford University Press, 1998).

92. Schmidt, K. & Atkinson, A. Feeding and Food Processing in Antarctic Krill (*Euphausia superba* Dana). *Biol. Ecol. Antarct. Krill* 175–224 (2016) doi:10.1007/978-3-319-29279-3_5.

93. Pearre, S. Feeding by Chaetognatha: The Relation of Prey Size to Predator Size in Several Species. *Mar. Ecol. Prog. Ser.* **3**, 125–134 (1980).

94. Bone, Q., Carré, C. & Chang, P. Tunicate feeding filters. *J. Mar. Biol. Assoc. U. K.* **83**, 907–919 (2003).

95. Pauly, D. & Christensen, V. Primary production required to sustain global fisheries. *Nature* **374**, 255–257 (1995).

96. Taylor, W. D. Maximum growth rate, size and commonness in a community of bactivorous ciliates. *Oecologia* **36**, 263–272 (1978).

97. López-Urrutia, Á., Harris, R. P. & Smith, T. Predation by calanoid copepods on the appendicularian *Oikopleura dioica*. *Limnol. Oceanogr.* **49**, 303–307 (2004).

98. Hopcroft, R. R., Roff, J. C. & Bouman, H. A. Zooplankton growth rates: the larvaceans Appendicularia, Fritillaria and Oikopleura in tropical waters. *J. Plankton Res.* **20**, 539–555 (1998).

99. Benedetti, F., Gasparini, S. & Ayata, S.-D. Identifying copepod functional groups from species functional traits. *J. Plankton Res.* **38**, 159–166 (2016).

100. Azevedo, F. de, Dias, J. D., Braghin, L. de S. M. & Bonecker, C. C. Length-weight regressions of the microcrustacean species from a tropical floodplain. *Acta Limnol. Bras.* **24**, 01–11 (2012).

101. Kawaguchi, S. *et al.* Will krill fare well under Southern Ocean acidification? *Biol. Lett.* **7**, 288–291 (2011).

102. Meyer, B. & Teschke, M. Physiology of *Euphausia superba*. *Biol. Ecol. Antarct. Krill* 145–174 (2016) doi:10.1007/978-3-319-29279-3_4.

103. Heron, A., McWilliam, P. & Dal Pont, G. Length-weight relation in the salp Thalia democratica and potential of salps as a source of food. *Mar. Ecol. Prog. Ser.* **42**, 125–132 (1988).

104. Acuña, J. L., López-Urrutia, Á. & Colin, S. Faking Giants: The Evolution of High Prey Clearance Rates in Jellyfishes. *Science* **333**, 1627–1629 (2011).

SUPPLEMENTARY MATERIAL

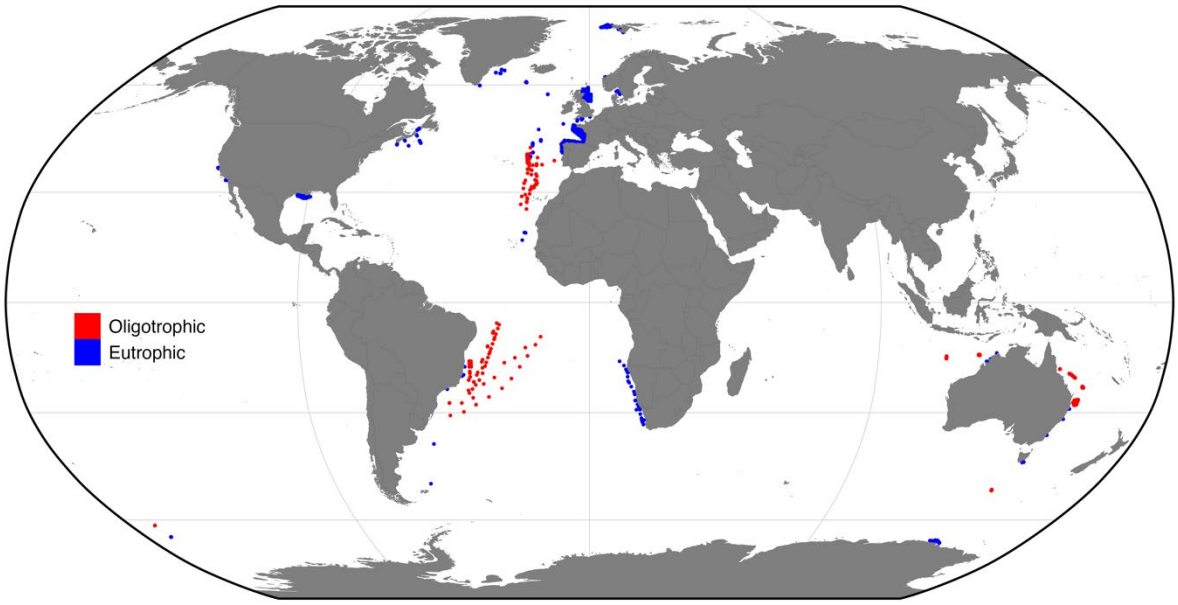

Figure S1: Observation locations for OPC/LOPC data

The location of OPC/LOPC observations used in the analysis, coloured by their nutrient status – Oligotrophic systems (red, Chlorophyll *a* < 0.1 mg m^{-3}) and Eutrophic (blue, Chlorophyll *a* > 1 mg m^{-3}).

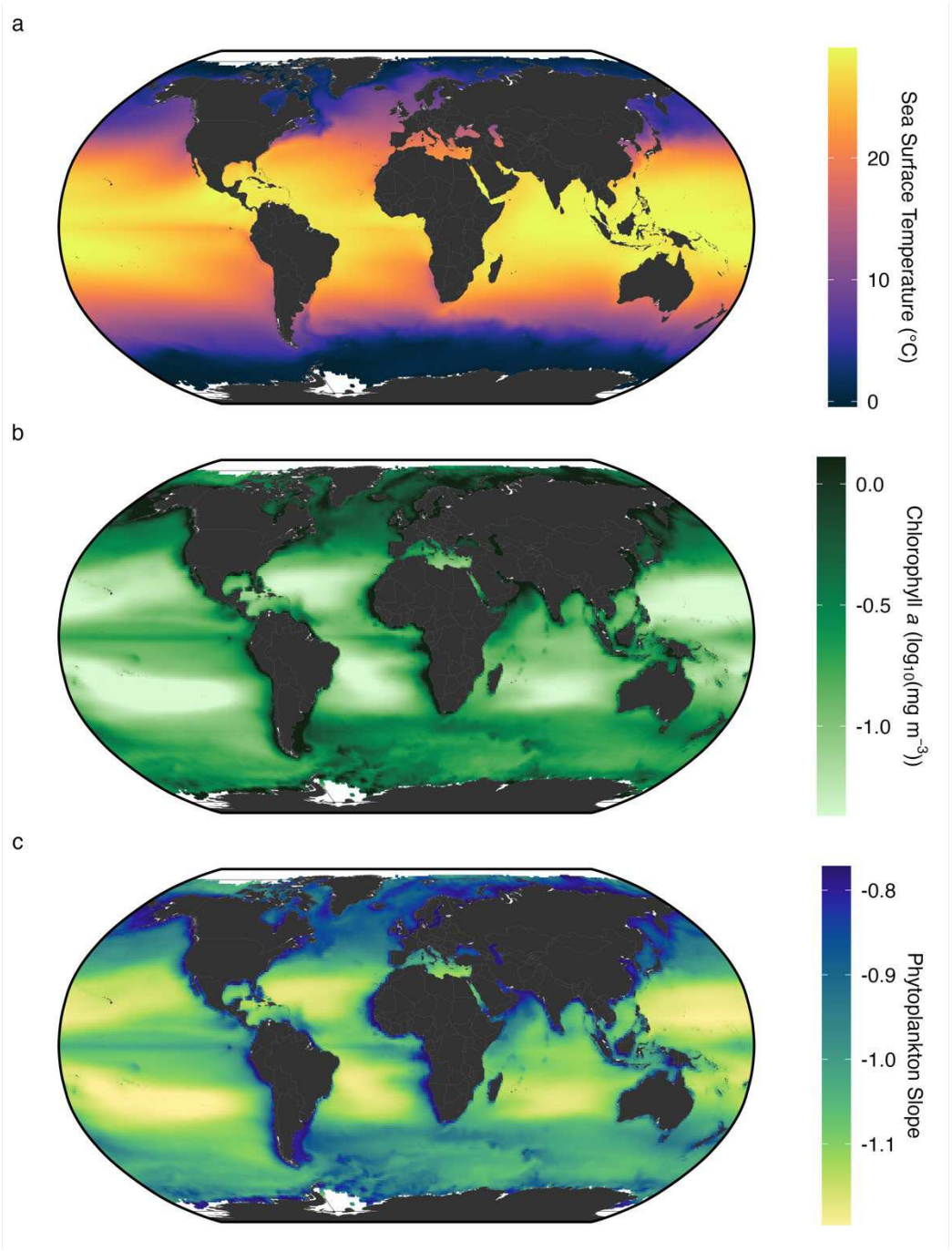

Figure S2: ZooMSS Environmental Inputs

a, Mean Sea Surface Temperature (°C), **b,** Mean Chlorophyll a (log_{10}(mg m^{-3})) and **c**, the slope of the phytoplankton size spectrum (derived from Chlorophyll *a*) in 1° cells (2002-2021) used as inputs to ZooMSS.

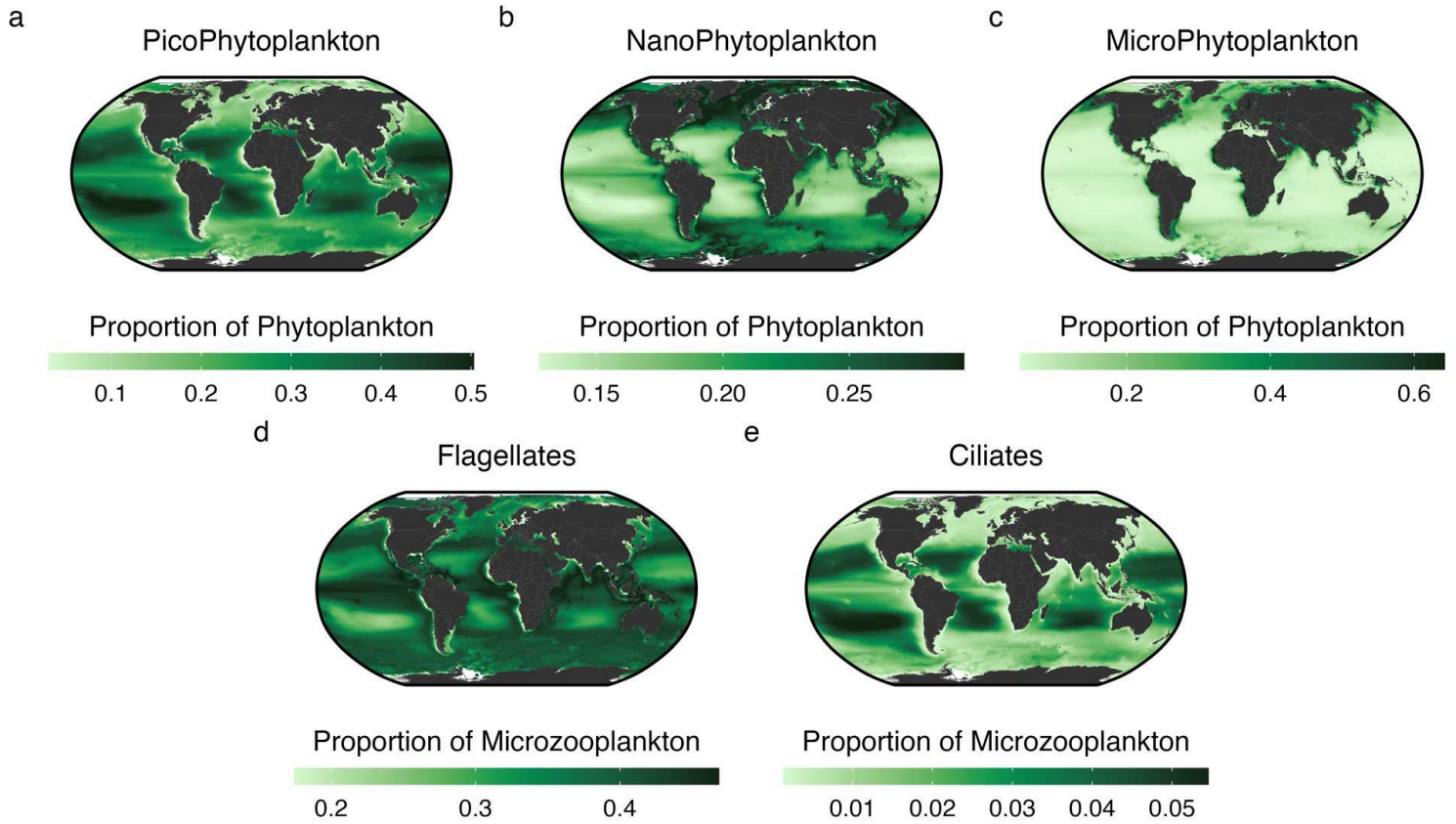

Figure S3: Distribution of phytoplankton and micro-zooplankton biomass in ZooMSS.

For each model cell, the relative proportion of **a,** pico-, **b,** nano- and **c,** micro-phytoplankton were calculated from empirical relationships based on chlorophyll *a* (Brewin et al. 2015) and used as model inputs. The proportion of micro-zooplankton (as model outputs) **d,** Flagellates and **e,** Ciliates are also shown.

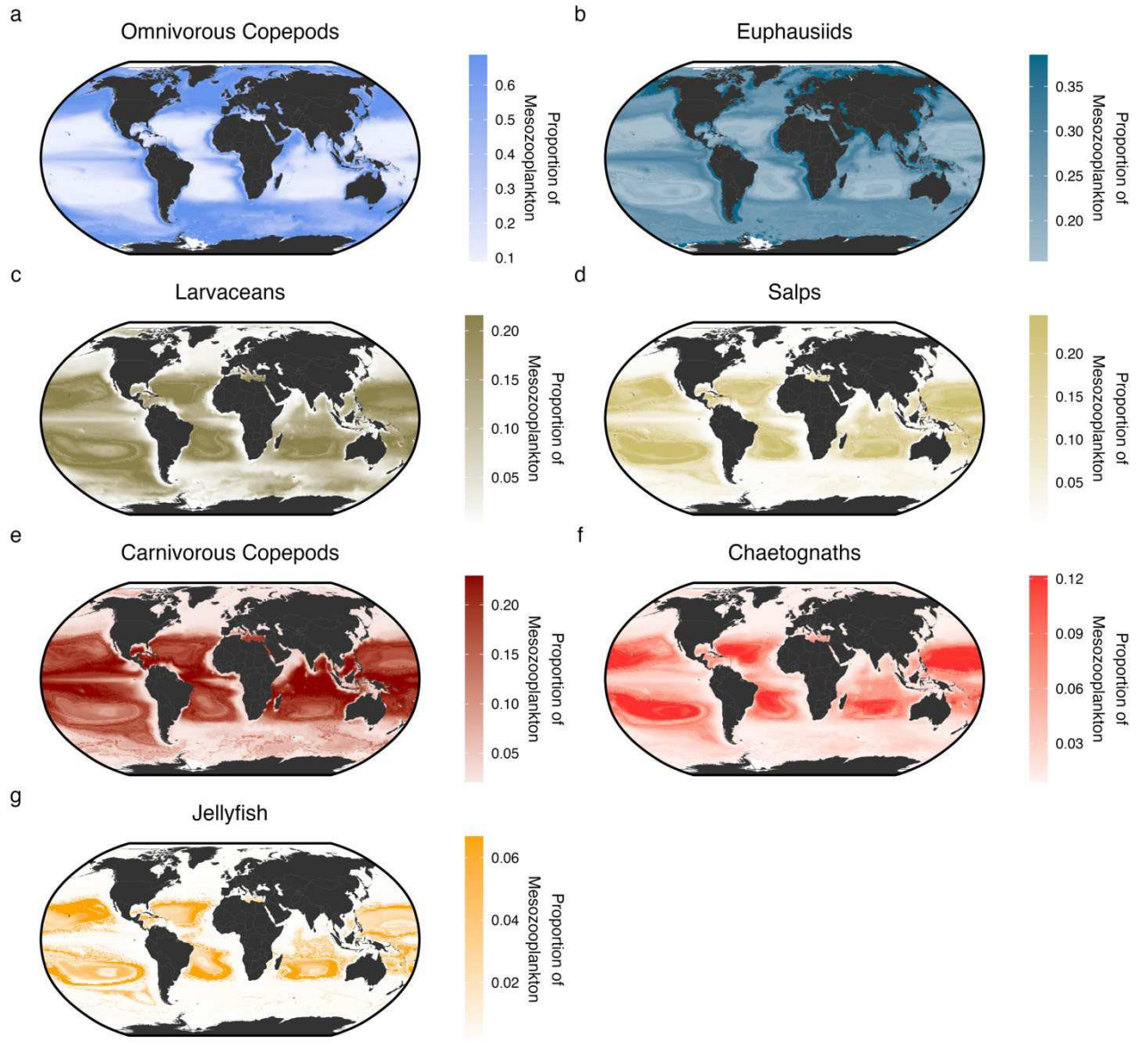

Figure S4: **Distribution of Mesozooplankton in ZooMSS.**

Output from ZooMSS showing proportional distribution of **a**, Omnivorous Copepods, **b**, Euphausiids, **c**, Larvaceans, **d**, Salps, **e**, Carnivorous Copepods, **f**, Chaetognaths, **g**, Jellyfish

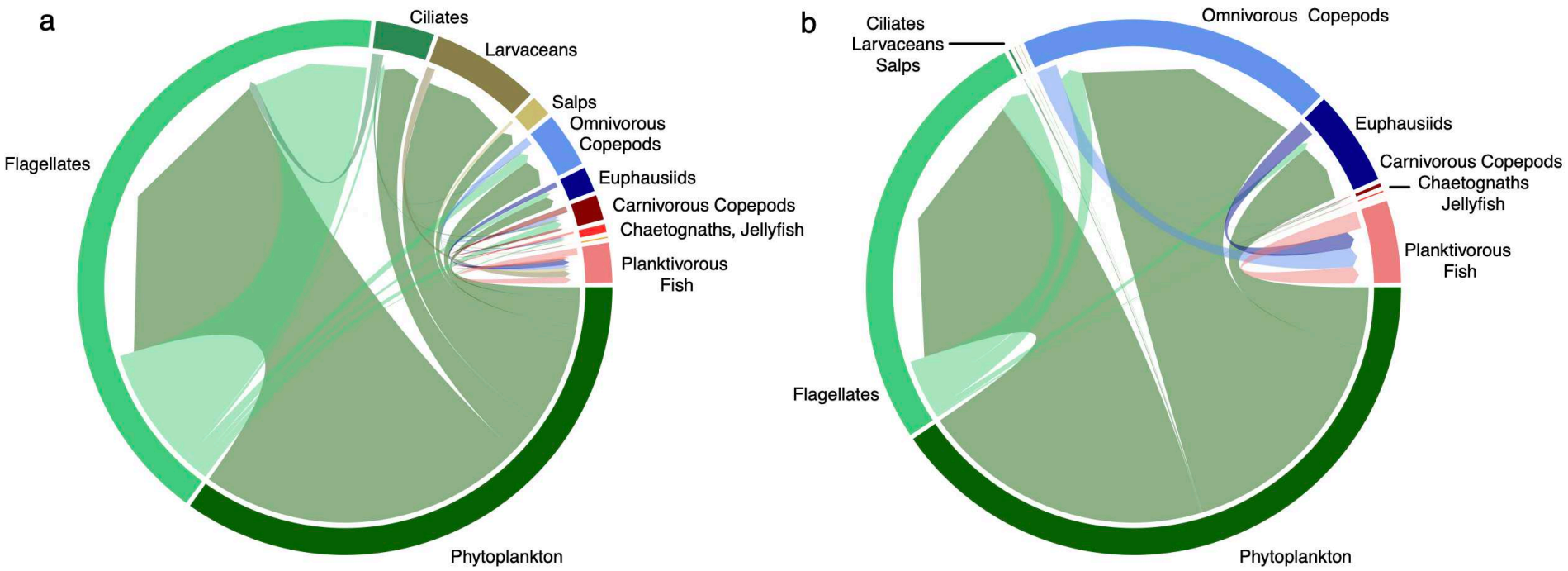

Figure S5: Output from ZooMSS showing food webs (including microzooplankton).

a, b, Circular food web diagrams showing biomass transfer in **(a)** Oligotrophic and **(b)** Eutrophic food webs. Pathways through the food web can be discerned by following the coloured link from the prey (outer colour) to their predator. The width of the link corresponds to the proportion of biomass of prey consumed by its predator, and the width of the outer band corresponds to the proportion of the model biomass.

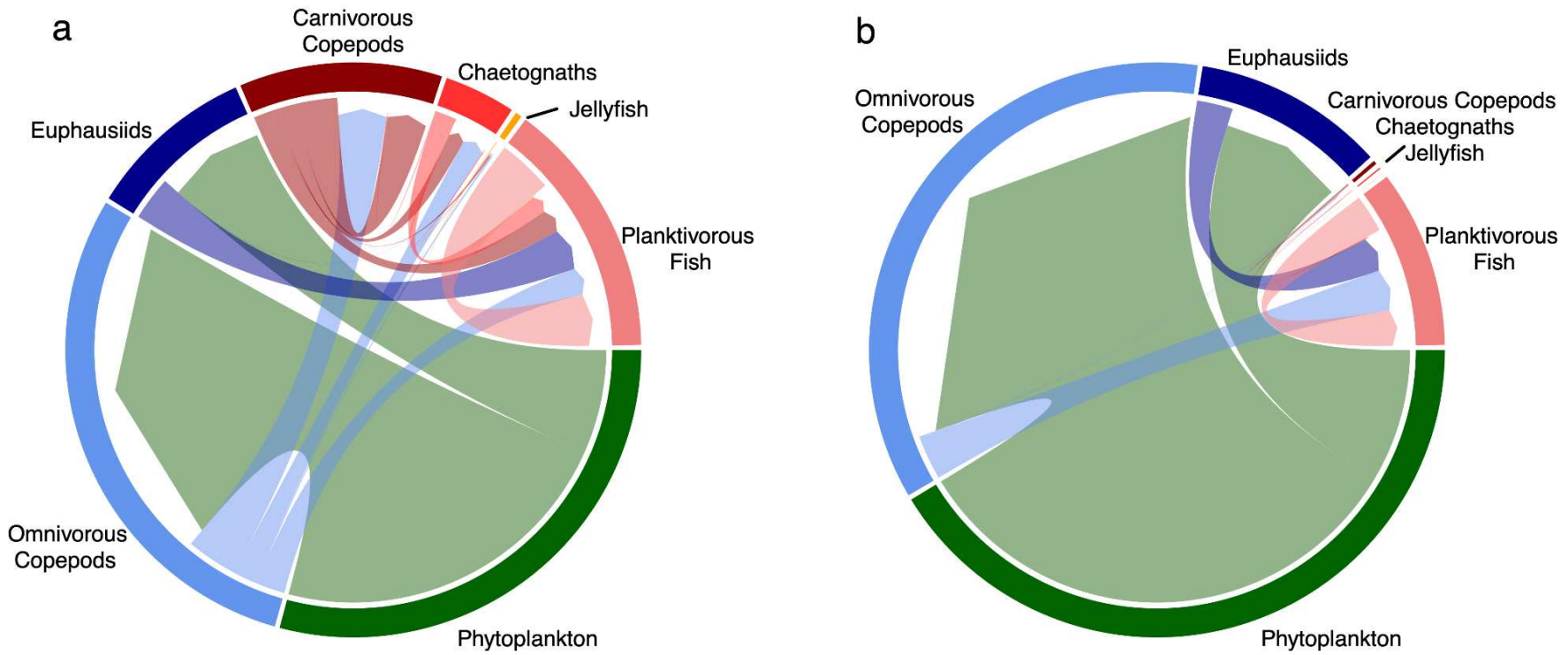

Figure S6: Output from ZooMSS showing food webs without Filter Feeders.

a, b, Circular food web diagrams showing biomass transfer in **(a)** Oligotrophic and **(b)** Eutrophic food webs when Filter Feeders are excluded. Pathways through the food web can be discerned by following the coloured link from the prey (outer colour) to their predator. The width of the link corresponds to the proportion of biomass of prey consumed by its predator, and the width of the outer band corresponds to the proportion of the model biomass. Compare figure with Figure 3a,b where all Mesozooplankton groups were included.

Table S1 Trait values for the nine zooplankton and three fish groups.

Group	**Min. Size, w_i**			**Max Size, $\underline{W_i}$**			**$\log_{10}$PPMR range, $\beta_i(w)$**	**Carbon-Wet Weight Ratio, C_i**
	Length	**ESD**	**$\log_{10}$(g)***	**Length**	**ESD**	**$\log_{10}$(g)***		
Hetero. Flagellates	-	3.3×10^{-4} cm[a]	–10.7[a]	-	7×10^{-3} cm[a]	–6.8[a]	0.2–0.7 [89]	0.15 [90]
Hetero. Ciliates	-	1×10^{-3} cm[b]	–9.3[b]	-	1×10^{-2} cm[b]	–6.3[a]	2.5–2.9 [89]	0.15 [90]
Larvaceans	8×10^{-3} cm[c]	1×10^{-2} cm[c]	–6.4[c]	3×10^{-1} cm[c]	1×10^{-1} cm[c]	–3.2[c]	6.8–10.8 [91]	0.02 [42]
Omni. Cop.	-	4×10^{-3} cm[d]	–7.5[d]	2.8×10^{-1} cm[e]	9×10^{-2} cm[e]	–3.5[e]	3.6–4.6 [89]	0.12 [79]
Carn. Cop.	-	4×10^{-3} cm[d]	–7.5[d]	6×10^{-1} cm[e]	1.8×10^{-1} cm[e]	–2.5[e]	0.8–1.9 [89]	0.12 [79]
Euphausiids	-	6×10^{-2} cm[f]	–4.2[f]	6 cm[g]	1.5 cm[g]	0.2[g]	6.6–7.8 [29,92]	0.12 [79]
Chaetognaths	1×10^{-1} cm[h]	1.5×10^{-2} cm[h]	–5.9[h]	4 cm[h]	6×10^{-1} cm[h]	–0.9[h]	1.9–3.4 [93]	0.04 [79]
Salps	5×10^{-2} cm[i]	5×10^{-2} cm[i]	–4.7[i]	-	3.6 cm[i]	1.4[i]	6.8–11.7 [94]	0.02 [42]
Jellyfish	-	1.2×10^{-1} cm[j]	–3[j]	-	6 cm[j]	2[j]	2.7–4.7 [79]	0.005 [79]
Small Fish	-	1.2×10^{-1} cm[k]	–3[k]	-	6 cm	2	2 [66]	0.1 [95]
Medium Fish	-	1.2×10^{-1} cm[k]	–3[k]	-	27 cm	4	2 [66]	0.1 [95]
Large Fish	-	1.2×10^{-1} cm[k]	–3[k]	-	125 cm	6	2 [66]	0.1 [95]

* g wet weight calculated from ESD, assuming 1 gram = 1 cm^3, ^ Feeding kernel widths were calculated with the empirical equation derived in Fuchs and Franks[29], using mean $\log_{10}$(PPMR) for this group.

[a] From Table 3 in Hansen et al.[79], [b] From figure 1 in Taylor[96], [c] Minimum and maximum larvacean trunk lengths taken from López-Urrutia[97] and Hopcroft et al.[98] respectively, and converted to ESD and wet weight using equation derived in Deibel[91], [d] Carbon mass obtained from supplementary material in Kiørboe and Hirst[80], converted to wet weight and ESD using carbon: wet weight ratio from Hansen et al.[79] [e] Maximum omnivorous and carnivorous copepod lengths taken from Benedetti et al.[99] and converted to ESD and then wet weight using equation derived in Azevedo et al.[100], [f] Euphausiid embryo ESD from figure 2 in Kawaguchi et al.[101], [g] Maximum length taken from supplementary material in Fuchs and Franks[29] and converted to ESD and wet weight using equation from Meyer and Teschke[102], [h] Minimum and maximum ESD from supplementary material in Fuchs and Franks[29], lengths derived using head-width:body-length ratio from Pearre [93], [i] Minimum and maximum salp length taken from Henschke et al.[38] and converted to ESD and wet weight using equation derived in Heron et al.[103], maximum salp body size taken as geometric mean of Salpida and Pyrosomatida from Henschke et al.[38], after using equation in Heron et al.[103], [j] From supplementary material in Acuña et al.[104], [k] From Heneghan et al.[67].